

Evidence for direct \mathcal{CP} violation in the measurement of the CKM angle γ with $B^\mp \rightarrow D^{(*)} K^{(*)\mp}$ decays

- P. del Amo Sanchez,¹ J. P. Lees,¹ V. Poireau,¹ E. Prencipe,¹ V. Tisserand,¹ J. Garra Tico,² E. Grauges,² M. Martinelli^{ab},³ A. Palano^{ab},³ M. Pappagallo^{ab},³ G. Eigen,⁴ B. Stugu,⁴ L. Sun,⁴ M. Battaglia,⁵ D. N. Brown,⁵ B. Hooberman,⁵ L. T. Kerth,⁵ Yu. G. Kolomensky,⁵ G. Lynch,⁵ I. L. Osipenkov,⁵ T. Tanabe,⁵ C. M. Hawkes,⁶ A. T. Watson,⁶ H. Koch,⁷ T. Schroeder,⁷ D. J. Asgeirsson,⁸ C. Hearty,⁸ T. S. Mattison,⁸ J. A. McKenna,⁸ A. Khan,⁹ A. Randle-Conde,⁹ V. E. Blinov,¹⁰ A. R. Buzykaev,¹⁰ V. P. Druzhinin,¹⁰ V. B. Golubev,¹⁰ A. P. Onuchin,¹⁰ S. I. Serednyakov,¹⁰ Yu. I. Skovpen,¹⁰ E. P. Solodov,¹⁰ K. Yu. Todyshev,¹⁰ A. N. Yushkov,¹⁰ M. Bondioli,¹¹ S. Curry,¹¹ D. Kirkby,¹¹ A. J. Lankford,¹¹ M. Mandelkern,¹¹ E. C. Martin,¹¹ D. P. Stoker,¹¹ H. Atmacan,¹² J. W. Gary,¹² F. Liu,¹² O. Long,¹² G. M. Vitug,¹² C. Campagnari,¹³ T. M. Hong,¹³ D. Kovalskyi,¹³ J. D. Richman,¹³ A. M. Eisner,¹⁴ C. A. Heusch,¹⁴ J. Kroseberg,¹⁴ W. S. Lockman,¹⁴ A. J. Martinez,¹⁴ T. Schalk,¹⁴ B. A. Schumm,¹⁴ A. Seiden,¹⁴ L. O. Winstrom,¹⁴ C. H. Cheng,¹⁵ D. A. Doll,¹⁵ B. Echenard,¹⁵ D. G. Hitlin,¹⁵ P. Ongmongkolkul,¹⁵ F. C. Porter,¹⁵ A. Y. Rakitin,¹⁵ R. Andreassen,¹⁶ M. S. Dubrovin,¹⁶ G. Mancinelli,¹⁶ B. T. Meadows,¹⁶ M. D. Sokoloff,¹⁶ P. C. Bloom,¹⁷ W. T. Ford,¹⁷ A. Gaz,¹⁷ J. F. Hirschauer,¹⁷ M. Nagel,¹⁷ U. Nauenberg,¹⁷ J. G. Smith,¹⁷ S. R. Wagner,¹⁷ R. Ayad,^{18,*} W. H. Toki,¹⁸ T. M. Karbach,¹⁹ J. Merkel,¹⁹ A. Petzold,¹⁹ B. Spaan,¹⁹ K. Wacker,¹⁹ M. J. Kobel,²⁰ K. R. Schubert,²⁰ R. Schwierz,²⁰ D. Bernard,²¹ M. Verderi,²¹ P. J. Clark,²² S. Playfer,²² J. E. Watson,²² M. Andreotti^{ab},²³ D. Bettoni^a,²³ C. Bozzi^a,²³ R. Calabrese^{ab},²³ A. Cecchi^{ab},²³ G. Cibinetto^{ab},²³ E. Fioravanti^{ab},²³ P. Franchini^{ab},²³ E. Luppi^{ab},²³ M. Munerato^{ab},²³ M. Negrini^{ab},²³ A. Petrella^{ab},²³ L. Piemontese^a,²³ R. Baldini-Ferroli,²⁴ A. Calcaterra,²⁴ R. de Sangro,²⁴ G. Finocchiaro,²⁴ M. Nicolaci,²⁴ S. Pacetti,²⁴ P. Patteri,²⁴ I. M. Peruzzi,^{24,†} M. Piccolo,²⁴ M. Rama,²⁴ A. Zallo,²⁴ R. Contri^{ab},²⁵ E. Guido^{ab},²⁵ M. Lo Vetere^{ab},²⁵ M. R. Monge^{ab},²⁵ S. Passaggio^a,²⁵ C. Patrignani^{ab},²⁵ E. Robutti^a,²⁵ S. Tosi^{ab},²⁵ B. Bhuyan,²⁶ M. Morii,²⁷ A. Adametz,²⁸ J. Marks,²⁸ S. Schenk,²⁸ U. Uwer,²⁸ F. U. Bernlochner,²⁹ H. M. Lacker,²⁹ T. Lueck,²⁹ A. Volk,²⁹ P. D. Dauncey,³⁰ M. Tibbetts,³⁰ P. K. Behera,³¹ U. Mallik,³¹ C. Chen,³² J. Cochran,³² H. B. Crawley,³² L. Dong,³² W. T. Meyer,³² S. Prell,³² E. I. Rosenberg,³² A. E. Rubin,³² Y. Y. Gao,³³ A. V. Gritsan,³³ Z. J. Guo,³³ N. Arnaud,³⁴ M. Davier,³⁴ D. Derkach,³⁴ J. Firmino da Costa,³⁴ G. Grosdidier,³⁴ F. Le Diberder,³⁴ A. M. Lutz,³⁴ B. Malaescu,³⁴ A. Perez,³⁴ P. Roudeau,³⁴ M. H. Schune,³⁴ J. Serrano,³⁴ V. Sordini,^{34,‡} A. Stocchi,³⁴ L. Wang,³⁴ G. Wormser,³⁴ D. J. Lange,³⁵ D. M. Wright,³⁵ I. Bingham,³⁶ J. P. Burke,³⁶ C. A. Chavez,³⁶ J. P. Coleman,³⁶ J. R. Fry,³⁶ E. Gabathuler,³⁶ R. Gamet,³⁶ D. E. Hutchcroft,³⁶ D. J. Payne,³⁶ C. Touramanis,³⁶ A. J. Bevan,³⁷ F. Di Lodovico,³⁷ R. Sacco,³⁷ M. Sigamani,³⁷ G. Cowan,³⁸ S. Paramesvaran,³⁸ A. C. Wren,³⁸ D. N. Brown,³⁹ C. L. Davis,³⁹ A. G. Denig,⁴⁰ M. Fritsch,⁴⁰ W. Gradl,⁴⁰ A. Hafner,⁴⁰ K. E. Alwyn,⁴¹ D. Bailey,⁴¹ R. J. Barlow,⁴¹ G. Jackson,⁴¹ G. D. Lafferty,⁴¹ T. J. West,⁴¹ J. Anderson,⁴² R. Cenci,⁴² A. Jawahery,⁴² D. A. Roberts,⁴² G. Simi,⁴² J. M. Tuggle,⁴² C. Dallapiccola,⁴³ E. Salvati,⁴³ R. Cowan,⁴⁴ D. Dujmic,⁴⁴ P. H. Fisher,⁴⁴ G. Sciolla,⁴⁴ M. Zhao,⁴⁴ D. Lindemann,⁴⁵ P. M. Patel,⁴⁵ S. H. Robertson,⁴⁵ M. Schram,⁴⁵ P. Biassoni^{ab},⁴⁶ A. Lazzaro^{ab},⁴⁶ V. Lombardo^a,⁴⁶ F. Palombo^{ab},⁴⁶ S. Stracka^{ab},⁴⁶ L. Cremaldi,⁴⁷ R. Godang,^{47,§} R. Kroeger,⁴⁷ P. Sonnek,⁴⁷ D. J. Summers,⁴⁷ H. W. Zhao,⁴⁷ X. Nguyen,⁴⁸ M. Simard,⁴⁸ P. Taras,⁴⁸ G. De Nardo^{ab},⁴⁹ D. Monorchio^{ab},⁴⁹ G. Onorato^{ab},⁴⁹ C. Sciacca^{ab},⁴⁹ G. Raven,⁵⁰ H. L. Snoek,⁵⁰ C. P. Jessop,⁵¹ K. J. Knoepfel,⁵¹ J. M. LoSecco,⁵¹ W. F. Wang,⁵¹ L. A. Corwin,⁵² K. Honscheid,⁵² R. Kass,⁵² J. P. Morris,⁵² A. M. Rahimi,⁵² N. L. Blount,⁵³ J. Brau,⁵³ R. Frey,⁵³ O. Igonkina,⁵³ J. A. Kolb,⁵³ R. Rahmat,⁵³ N. B. Sinev,⁵³ D. Strom,⁵³ J. Strube,⁵³ E. Torrence,⁵³ G. Castellini^{ab},⁵⁴ E. Feltresi^{ab},⁵⁴ N. Gagliardi^{ab},⁵⁴ M. Margoni^{ab},⁵⁴ M. Morandin^a,⁵⁴ M. Posocco^a,⁵⁴ M. Rotondo^a,⁵⁴ F. Simonetto^{ab},⁵⁴ R. Stroili^{ab},⁵⁴ E. Ben-Haim,⁵⁵ G. R. Bonneauaud,⁵⁵ H. Briand,⁵⁵ G. Calderini,⁵⁵ J. Chauveau,⁵⁵ O. Hamon,⁵⁵ Ph. Leruste,⁵⁵ G. Marchiori,⁵⁵ J. Ocariz,⁵⁵ J. Prendki,⁵⁵ S. Sitt,⁵⁵ M. Biasini^{ab},⁵⁶ E. Manoni^{ab},⁵⁶ C. Angelini^{ab},⁵⁷ G. Batignani^{ab},⁵⁷ S. Bettarini^{ab},⁵⁷ M. Carpinelli^{ab},⁵⁷ ¶ G. Casarosa^{ab},⁵⁷ A. Cervelli^{ab},⁵⁷ F. Forti^{ab},⁵⁷ M. A. Giorgi^{ab},⁵⁷ A. Lusiani^{ac},⁵⁷ N. Neri^{ab},⁵⁷ E. Paoloni^{ab},⁵⁷ G. Rizzo^{ab},⁵⁷ J. J. Walsh^a,⁵⁷ D. Lopes Pegna,⁵⁸ C. Lu,⁵⁸ J. Olsen,⁵⁸ A. J. S. Smith,⁵⁸ A. V. Telnov,⁵⁸ F. Anulli^a,⁵⁹ E. Baracchini^{ab},⁵⁹ G. Cavoto^a,⁵⁹ R. Faccini^{ab},⁵⁹ F. Ferrarotto^a,⁵⁹ F. Ferroni^{ab},⁵⁹ M. Gaspero^{ab},⁵⁹ L. Li Gioi^a,⁵⁹ M. A. Mazzoni^a,⁵⁹ G. Piredda^a,⁵⁹ F. Renga^{ab},⁵⁹ M. Ebert,⁶⁰ T. Hartmann,⁶⁰ T. Leddig,⁶⁰ H. Schröder,⁶⁰ R. Waldi,⁶⁰ T. Adye,⁶¹ B. Franek,⁶¹ E. O. Olaiya,⁶¹ F. F. Wilson,⁶¹ S. Emery,⁶² G. Hamel de Monchenault,⁶² G. Vasseur,⁶² Ch. Yéche,⁶² M. Zito,⁶² I. J. R. Aitchison,^{63, **}

M. T. Allen,⁶³ D. Aston,⁶³ D. J. Bard,⁶³ R. Bartoldus,⁶³ J. F. Benitez,⁶³ C. Cartaro,⁶³ M. R. Convery,⁶³ J. Dorfan,⁶³ G. P. Dubois-Felsmann,⁶³ W. Dunwoodie,⁶³ R. C. Field,⁶³ M. Franco Sevilla,⁶³ B. G. Fulsom,⁶³ A. M. Gabareen,⁶³ M. T. Graham,⁶³ P. Grenier,⁶³ C. Hast,⁶³ W. R. Innes,⁶³ M. H. Kelsey,⁶³ H. Kim,⁶³ P. Kim,⁶³ M. L. Kocian,⁶³ D. W. G. S. Leith,⁶³ S. Li,⁶³ B. Lindquist,⁶³ S. Luitz,⁶³ V. Luth,⁶³ H. L. Lynch,⁶³ D. B. MacFarlane,⁶³ H. Marsiske,⁶³ D. R. Muller,⁶³ H. Neal,⁶³ S. Nelson,⁶³ C. P. O'Grady,⁶³ I. Ofte,⁶³ M. Perl,⁶³ T. Pulliam,⁶³ B. N. Ratcliff,⁶³ A. Roodman,⁶³ A. A. Salnikov,⁶³ V. Santoro,⁶³ R. H. Schindler,⁶³ J. Schwiening,⁶³ A. Snyder,⁶³ D. Su,⁶³ M. K. Sullivan,⁶³ S. Sun,⁶³ K. Suzuki,⁶³ J. M. Thompson,⁶³ J. Va'vra,⁶³ A. P. Wagner,⁶³ M. Weaver,⁶³ C. A. West,⁶³ W. J. Wisniewski,⁶³ M. Wittgen,⁶³ D. H. Wright,⁶³ H. W. Wulsin,⁶³ A. K. Yarritu,⁶³ C. C. Young,⁶³ V. Ziegler,⁶³ X. R. Chen,⁶⁴ W. Park,⁶⁴ M. V. Purohit,⁶⁴ R. M. White,⁶⁴ J. R. Wilson,⁶⁴ S. J. Sekula,⁶⁵ M. Bellis,⁶⁶ P. R. Burchat,⁶⁶ A. J. Edwards,⁶⁶ T. S. Miyashita,⁶⁶ S. Ahmed,⁶⁷ M. S. Alam,⁶⁷ J. A. Ernst,⁶⁷ B. Pan,⁶⁷ M. A. Saeed,⁶⁷ S. B. Zain,⁶⁷ N. Guttmann,⁶⁸ A. Soffer,⁶⁸ P. Lund,⁶⁹ S. M. Spanier,⁶⁹ R. Eckmann,⁷⁰ J. L. Ritchie,⁷⁰ A. M. Ruland,⁷⁰ C. J. Schilling,⁷⁰ R. F. Schwitters,⁷⁰ B. C. Wray,⁷⁰ J. M. Izen,⁷¹ X. C. Lou,⁷¹ F. Bianchi^{ab},⁷² D. Gamba^{ab},⁷² M. Pelliccioni^{ab},⁷² M. Bomben^{ab},⁷³ L. Lanceri^{ab},⁷³ L. Vitale^{ab},⁷³ N. Lopez-March,⁷⁴ F. Martinez-Vidal,⁷⁴ D. A. Milanes,⁷⁴ A. Oyanguren,⁷⁴ J. Albert,⁷⁵ Sw. Banerjee,⁷⁵ H. H. F. Choi,⁷⁵ K. Hamano,⁷⁵ G. J. King,⁷⁵ R. Kowalewski,⁷⁵ M. J. Lewczuk,⁷⁵ I. M. Nugent,⁷⁵ J. M. Roney,⁷⁵ R. J. Sobie,⁷⁵ T. J. Gershon,⁷⁶ P. F. Harrison,⁷⁶ J. Illic,⁷⁶ T. E. Latham,⁷⁶ E. M. T. Puccio,⁷⁶ H. R. Band,⁷⁷ X. Chen,⁷⁷ S. Dasu,⁷⁷ K. T. Flood,⁷⁷ Y. Pan,⁷⁷ R. Prepost,⁷⁷ C. O. Vuosalo,⁷⁷ and S. L. Wu⁷⁷

(The BABAR Collaboration)

¹Laboratoire d'Annecy-le-Vieux de Physique des Particules (LAPP),

Université de Savoie, CNRS/IN2P3, F-74941 Annecy-Le-Vieux, France

²Universitat de Barcelona, Facultat de Fisica, Departament ECM, E-08028 Barcelona, Spain

³INFN Sezione di Bari^a; Dipartimento di Fisica, Università di Bari^b, I-70126 Bari, Italy

⁴University of Bergen, Institute of Physics, N-50007 Bergen, Norway

⁵Lawrence Berkeley National Laboratory and University of California, Berkeley, California 94720, USA

⁶University of Birmingham, Birmingham, B15 2TT, United Kingdom

⁷Ruhr Universität Bochum, Institut für Experimentalphysik 1, D-44780 Bochum, Germany

⁸University of British Columbia, Vancouver, British Columbia, Canada V6T 1Z1

⁹Brunel University, Uxbridge, Middlesex UB8 3PH, United Kingdom

¹⁰Budker Institute of Nuclear Physics, Novosibirsk 630090, Russia

¹¹University of California at Irvine, Irvine, California 92697, USA

¹²University of California at Riverside, Riverside, California 92521, USA

¹³University of California at Santa Barbara, Santa Barbara, California 93106, USA

¹⁴University of California at Santa Cruz, Institute for Particle Physics, Santa Cruz, California 95064, USA

¹⁵California Institute of Technology, Pasadena, California 91125, USA

¹⁶University of Cincinnati, Cincinnati, Ohio 45221, USA

¹⁷University of Colorado, Boulder, Colorado 80309, USA

¹⁸Colorado State University, Fort Collins, Colorado 80523, USA

¹⁹Technische Universität Dortmund, Fakultät Physik, D-44221 Dortmund, Germany

²⁰Technische Universität Dresden, Institut für Kern- und Teilchenphysik, D-01062 Dresden, Germany

²¹Laboratoire Leprince-Ringuet, CNRS/IN2P3, Ecole Polytechnique, F-91128 Palaiseau, France

²²University of Edinburgh, Edinburgh EH9 3JZ, United Kingdom

²³INFN Sezione di Ferrara^a; Dipartimento di Fisica, Università di Ferrara^b, I-44100 Ferrara, Italy

²⁴INFN Laboratori Nazionali di Frascati, I-00044 Frascati, Italy

²⁵INFN Sezione di Genova^a; Dipartimento di Fisica, Università di Genova^b, I-16146 Genova, Italy

²⁶Indian Institute of Technology Guwahati, Guwahati, Assam, 781 039, India

²⁷Harvard University, Cambridge, Massachusetts 02138, USA

²⁸Universität Heidelberg, Physikalisches Institut, Philosophenweg 12, D-69120 Heidelberg, Germany

²⁹Humboldt-Universität zu Berlin, Institut für Physik, Newtonstr. 15, D-12489 Berlin, Germany

³⁰Imperial College London, London, SW7 2AZ, United Kingdom

³¹University of Iowa, Iowa City, Iowa 52242, USA

³²Iowa State University, Ames, Iowa 50011-3160, USA

³³Johns Hopkins University, Baltimore, Maryland 21218, USA

³⁴Laboratoire de l'Accélérateur Linéaire, IN2P3/CNRS et Université Paris-Sud 11,

Centre Scientifique d'Orsay, B. P. 34, F-91898 Orsay Cedex, France

³⁵Lawrence Livermore National Laboratory, Livermore, California 94550, USA

³⁶University of Liverpool, Liverpool L69 7ZE, United Kingdom

³⁷Queen Mary, University of London, London, E1 4NS, United Kingdom

³⁸University of London, Royal Holloway and Bedford New College, Egham, Surrey TW20 0EX, United Kingdom

³⁹University of Louisville, Louisville, Kentucky 40292, USA

- ⁴⁰Johannes Gutenberg-Universität Mainz, Institut für Kernphysik, D-55099 Mainz, Germany
⁴¹University of Manchester, Manchester M13 9PL, United Kingdom
⁴²University of Maryland, College Park, Maryland 20742, USA
⁴³University of Massachusetts, Amherst, Massachusetts 01003, USA
⁴⁴Massachusetts Institute of Technology, Laboratory for Nuclear Science, Cambridge, Massachusetts 02139, USA
⁴⁵McGill University, Montréal, Québec, Canada H3A 2T8
⁴⁶INFN Sezione di Milano^a; Dipartimento di Fisica, Università di Milano^b, I-20133 Milano, Italy
⁴⁷University of Mississippi, University, Mississippi 38677, USA
⁴⁸Université de Montréal, Physique des Particules, Montréal, Québec, Canada H3C 3J7
⁴⁹INFN Sezione di Napoli^a; Dipartimento di Scienze Fisiche, Università di Napoli Federico II^b, I-80126 Napoli, Italy
⁵⁰NIKHEF, National Institute for Nuclear Physics and High Energy Physics, NL-1009 DB Amsterdam, The Netherlands
⁵¹University of Notre Dame, Notre Dame, Indiana 46556, USA
⁵²Ohio State University, Columbus, Ohio 43210, USA
⁵³University of Oregon, Eugene, Oregon 97403, USA
⁵⁴INFN Sezione di Padova^a; Dipartimento di Fisica, Università di Padova^b, I-35131 Padova, Italy
⁵⁵Laboratoire de Physique Nucléaire et de Hautes Energies, IN2P3/CNRS, Université Pierre et Marie Curie-Paris6, Université Denis Diderot-Paris7, F-75252 Paris, France
⁵⁶INFN Sezione di Perugia^a; Dipartimento di Fisica, Università di Perugia^b, I-06100 Perugia, Italy
⁵⁷INFN Sezione di Pisa^a; Dipartimento di Fisica, Università di Pisa^b; Scuola Normale Superiore di Pisa^c, I-56127 Pisa, Italy
⁵⁸Princeton University, Princeton, New Jersey 08544, USA
⁵⁹INFN Sezione di Roma^a; Dipartimento di Fisica, Università di Roma La Sapienza^b, I-00185 Roma, Italy
⁶⁰Universität Rostock, D-18051 Rostock, Germany
⁶¹Rutherford Appleton Laboratory, Chilton, Didcot, Oxon, OX11 0QX, United Kingdom
⁶²CEA, Irfu, SPP, Centre de Saclay, F-91191 Gif-sur-Yvette, France
⁶³SLAC National Accelerator Laboratory, Stanford, California 94309 USA
⁶⁴University of South Carolina, Columbia, South Carolina 29208, USA
⁶⁵Southern Methodist University, Dallas, Texas 75275, USA
⁶⁶Stanford University, Stanford, California 94305-4060, USA
⁶⁷State University of New York, Albany, New York 12222, USA
⁶⁸Tel Aviv University, School of Physics and Astronomy, Tel Aviv, 69978, Israel
⁶⁹University of Tennessee, Knoxville, Tennessee 37996, USA
⁷⁰University of Texas at Austin, Austin, Texas 78712, USA
⁷¹University of Texas at Dallas, Richardson, Texas 75083, USA
⁷²INFN Sezione di Torino^a; Dipartimento di Fisica Sperimentale, Università di Torino^b, I-10125 Torino, Italy
⁷³INFN Sezione di Trieste^a; Dipartimento di Fisica, Università di Trieste^b, I-34127 Trieste, Italy
⁷⁴IFIC, Universitat de Valencia-CSIC, E-46071 Valencia, Spain
⁷⁵University of Victoria, Victoria, British Columbia, Canada V8W 3P6
⁷⁶Department of Physics, University of Warwick, Coventry CV4 7AL, United Kingdom
⁷⁷University of Wisconsin, Madison, Wisconsin 53706, USA

(Dated: October 26, 2018)

We report the measurement of the Cabibbo-Kobayashi-Maskawa CP -violating angle γ through a Dalitz plot analysis of neutral D meson decays to $K_S^0\pi^+\pi^-$ and $K_S^0K^+K^-$ produced in the processes $B^\mp \rightarrow DK^\mp$, $B^\mp \rightarrow D^*K^\mp$ with $D^* \rightarrow D\pi^0$, $D\gamma$, and $B^\mp \rightarrow DK^{*\mp}$ with $K^{*\mp} \rightarrow K_S^0\pi^\mp$, using 468 million $B\bar{B}$ pairs collected by the BABAR detector at the PEP-II asymmetric-energy e^+e^- collider at SLAC. We measure $\gamma = (68 \pm 14 \pm 4 \pm 3)^\circ$ (modulo 180°), where the first error is statistical, the second is the experimental systematic uncertainty and the third reflects the uncertainty in the description of the neutral D decay amplitudes. This result is inconsistent with $\gamma = 0$ (no direct CP violation) with a significance of 3.5 standard deviations.

PACS numbers: 13.25.Hw, 11.30.Er, 12.15.Hh, 13.25.Ft

The breaking of the CP symmetry in the quark sector of the electroweak interactions arises in the standard model (SM) from a single irreducible phase in the Cabibbo-Kobayashi-Maskawa (CKM) quark-mixing matrix [1]. This phase can be measured using a variety of methods involving B -meson decays mediated by either

only tree-level or both tree- and loop-level amplitudes. The comparison of these two classes of measurements tests the CKM mechanism, thus offering a strategy to search for new physics [2]. The angle γ of the unitarity triangle, defined as $\arg[-V_{ud}V_{ub}^*/V_{cd}V_{cb}^*]$, where V_{ij} are elements of the CKM matrix, is particularly relevant

since it is the only CP -violating parameter that can be cleanly determined using solely tree-level B -meson decays. Its precise determination constitutes an important goal of present and future experiments in flavor physics.

In $B^\mp \rightarrow DK^\mp$ decays [3, 4] the color-favored $B^- \rightarrow D^0 K^-$ ($b \rightarrow c\bar{s}$) and the color-suppressed $B^- \rightarrow \bar{D}^0 K^-$ ($b \rightarrow u\bar{s}$) transitions [5] interfere when the D^0 and \bar{D}^0 decay to a common final state [6]. The two interfering amplitudes differ by a factor $r_B e^{i(\delta_B \mp \gamma)}$, where r_B is the magnitude of the ratio of the amplitudes $\mathcal{A}(B^- \rightarrow \bar{D}^0 K^-)$ and $\mathcal{A}(B^- \rightarrow D^0 K^-)$, and δ_B is their relative strong phase. An amplitude analysis of the Dalitz plot (DP) of D^0 and \bar{D}^0 mesons decaying into the $K_s^0 \pi^+ \pi^-$ and $K_s^0 K^+ K^-$ self-conjugate final states from $B^\mp \rightarrow DK^\mp$ decays offers a unique way to access the complex amplitude ratios and thus the weak and strong phases, and r_B . The experimental sensitivity to γ arises mostly from regions in the DP where Cabibbo-favored (CF) and doubly-Cabibbo-suppressed (DCS) amplitudes interfere, and from regions populated by CP eigenstates, thus the uncertainty on γ depends on $1/r_B$ ($r_B \sim 0.1 - 0.2$).

In this Letter we study the interference between color-favored and color-suppressed transitions as a function of the position in the DP of squared invariant masses $s_- = m^2(K_s^0 h^-)$, $s_+ = m^2(K_s^0 h^+)$, where h represents π or K , for three related B decays, $B^\mp \rightarrow DK^\mp$, $B^\mp \rightarrow D^* K^\mp$, and $B^\mp \rightarrow DK^{*\mp}$ [4, 7], and report the most precise single measurement of the complex amplitude ratios and evidence for direct CP violation. We use the complete data sample of 425 fb^{-1} of integrated luminosity at the $\Upsilon(4S)$, corresponding to $468 \times 10^6 B\bar{B}$ pairs, and 45 fb^{-1} at a center-of-mass (c.m.) energy 40 MeV below the $\Upsilon(4S)$, recorded by the *BABAR* experiment [8] at the PEP-II asymmetric-energy $e^+ e^-$ collider at SLAC from 1999 to 2008. This measurement updates our previous results based on a partial sample of $383 \times 10^6 B\bar{B}$ pairs, from which we reported a significance of direct CP violation ($\gamma \neq 0$) of 3.0 standard deviations, while most of the analysis details remain unchanged [9]. The Belle Collaboration using $B^\mp \rightarrow D^{(*)} K^\mp$, $D \rightarrow K_s^0 \pi^+ \pi^-$ alone [10] has also reported $\gamma \neq 0$ with a significance of 3.5 standard deviations.

We reconstruct a total of eight signal samples, $B^\mp \rightarrow D^{(*)} K^\mp$ and $B^\mp \rightarrow DK^{*\mp}$, with $D^* \rightarrow D\pi^0$, $D\gamma$, $K^{*\mp} \rightarrow K_s^0 \pi^{\mp}$, with selection criteria nearly identical to our previous analysis. The $DK^{*\mp}$ final state, for $D \rightarrow K_s^0 K^+ K^-$, has been considered for the first time. For $K_s^0 \rightarrow \pi^+ \pi^-$ candidates, we further require the decay length (defined by the K_s^0 production and decay vertices) projected along the K_s^0 momentum to be greater than 10 times its error. This additional requirement helps to reduce to a negligible level background events from $D \rightarrow \pi^+ \pi^- h^+ h^-$ decays, and from $a_1(1260)^\mp$ misreconstructed as $K^{*\mp}$. After all the selection criteria the background is completely dominated by random

combinations of tracks arising from continuum events, $e^+ e^- \rightarrow q\bar{q}$ ($q = u, d, s$, or c). Background contributions from $D \rightarrow K_s^0 K_s^0$ decays are found to be negligible. The B^\mp candidates are characterized using the beam-energy substituted B mass m_{ES} , the difference between the reconstructed energy of the B^\mp candidate and the beam energy in the $e^+ e^-$ c.m. frame ΔE , and a Fisher discriminant \mathcal{F} that combines four topological variables optimized to separate continuum events [9]. We retain candidates with the loose requirements $m_{\text{ES}} > 5.2 \text{ GeV}/c^2$, $-80 < \Delta E < 120 \text{ MeV}$, and $|\mathcal{F}| < 1.4$, which provide signal and sideband regions while removing poorly reconstructed candidates [11]. The reconstruction efficiencies in a signal region with $m_{\text{ES}} > 5.272 \text{ GeV}/c^2$ and $|\Delta E| < 30 \text{ MeV}$ are 26%, 12%, 15%, and 14%, for the DK^\mp , $D^*[D\pi^0]K^\mp$, $D^*[D\gamma]K^\mp$, and $DK^{*\mp}$ final states, respectively, for $D \rightarrow K_s^0 \pi^+ \pi^-$ (and slightly lower for $D \rightarrow K_s^0 K^+ K^-$). These values are about 30%, 40%, 30%, and 20% larger than in our previous analysis, with similar background levels, reflecting improvements in tracking and particle identification. The m_{ES} , ΔE , \mathcal{F} , and (s_-, s_+) distributions for events in the signal region can be found in [11].

The $D^0 \rightarrow K_s^0 h^+ h^-$ decay amplitudes $\mathcal{A}(s_-, s_+)$ are determined using the same data sample through DP analyses of D^0 mesons from $D^{*+} \rightarrow D^0 \pi^+$ decays produced in $e^+ e^- \rightarrow c\bar{c}$ events [9, 12]. The charge of the low momentum π^+ from the D^{*+} decay identifies the flavor of the D meson. The signal purities of the samples are 98.5% and 99.2%, with about 541 000 and 80 000 candidates, for $K_s^0 \pi^+ \pi^-$ and $K_s^0 K^+ K^-$, respectively. The dynamical properties of the P- and D-wave amplitudes are parameterized through intermediate resonances with mass-dependent relativistic Breit-Wigner (BW) or Gounaris-Sakurai propagators, Blatt-Weisskopf centrifugal barrier factors, and Zemach tensors for the angular distributions [13]. The $\pi\pi$ S-wave dynamics is described through a K-matrix formalism with the P-vector approximation and 5 poles [9, 14]. For the $K\pi$ S-wave we include a BW for the $K_0^*(1430)^\mp$ state with a coherent non-resonant contribution parameterized by a scattering length and effective range similar to those used to describe $K\pi$ scattering data [15]. For the $K\bar{K}$ S-wave, a coupled-channel BW is used for the $a_0(980)$ with single BWs for $f_0(1370)$ and $a_0(1450)$ states. Overall, the amplitude models reproduce well the DP distributions [12]. MC studies show that a significant contribution to the discrepancies arise from imperfections modeling the efficiency variations at the boundaries of the DP and the invariant mass resolution. We account for these and other imperfections in the modeling of the D^0 decay amplitudes through our model systematic uncertainties.

We perform a simultaneous, unbinned, and extended maximum-likelihood fit (referred to as CP fit) to the $B^\mp \rightarrow D^{(*)} K^\mp$ and $B^\mp \rightarrow DK^{*\mp}$ decay rates $\Gamma_{\mp}^{(*)}$ and $\Gamma_{s\mp}$ as a function of m_{ES} , ΔE , \mathcal{F} , and (s_-, s_+) [9, 11].

We extract the signal and background yields, along with the CP -violating parameters $z_{\mp}^{(*)} \equiv x_{\mp}^{(*)} + iy_{\mp}^{(*)}$ and $z_{s\mp} \equiv x_{s\mp} + iy_{s\mp}$, defined as the B^{\mp} complex amplitude ratios $z_{\mp}^{(*)} = r_{B^{\mp}}^{(*)} e^{i(\delta_B^{(*)}) \mp \gamma}$ and $z_{s\mp} = \kappa r_{s\mp} e^{i(\delta_s \mp \gamma)}$, respectively. Here, $r_{B^{\mp}}^{(*)}$ and $r_{s\mp}$ are the corresponding magnitude ratios between the $b \rightarrow u$ and $b \rightarrow c$ amplitudes for B^{\mp} decays, $\delta_B^{(*)}$ and δ_s the relative strong phases, and κ an effective hadronic parameter that accounts for the interference between $B^{\mp} \rightarrow DK^{*\mp}$ and other $B^{\mp} \rightarrow DK_s^0 \pi^{\mp}$ decays, as a consequence of the $K^{*\mp}$ natural width [9, 16, 17]. Assuming no CP violation and neglecting $D^0 - \bar{D}^0$ mixing in $D^0 \rightarrow K_s^0 h^+ h^-$ decays [12, 18, 19], the relation $\bar{\mathcal{A}}(s_-, s_+) = \mathcal{A}(s_+, s_-)$ holds, where $\bar{\mathcal{A}}$ is the \bar{D}^0 decay amplitude. The $B^{\mp} \rightarrow D^{(*)} K^{\mp}$ (and similarly for $B^{\mp} \rightarrow DK^{*\mp}$ replacing $z_{\mp}^{(*)}$ and $r_{B^{\mp}}^{(*)}$ by $z_{s\mp}$ and $r_{s\mp}$, respectively) signal decay rates are then

$$\Gamma_{\mp}^{(*)}(s_-, s_+) \propto |\mathcal{A}_{\mp}|^2 + r_{B^{\mp}}^{(*)}{}^2 |\mathcal{A}_{\pm}|^2 + 2\lambda z_{\mp}^{(*)} \mathcal{A}_{\mp} \mathcal{A}_{\pm}^*,$$

with $\mathcal{A}_{\mp} \equiv \mathcal{A}(s_{\mp}, s_{\pm})$, and $\lambda = +1$ except for $B^{\mp} \rightarrow D^{*}[D\gamma]K^{\mp}$ where $\lambda = -1$ [20]. We apply corrections for efficiency variations and neglect the invariant mass resolution across the DP [9]. For each signal sample, the following background components are considered: continuum events, $B^{\mp} \rightarrow D^{(*)}\pi^{\mp}$ decays where the pion is misidentified as a kaon (only for $B^{\mp} \rightarrow D^{(*)}K^{\mp}$ samples), and $\Upsilon(4S) \rightarrow B\bar{B}$ (other than $B^{\mp} \rightarrow D^{(*)}\pi^{\mp}$) decays. The reference CP fit requires events to satisfy $|\Delta E| < 30$ MeV, but alternative fits are performed varying the requirements on the m_{ES} , ΔE , and \mathcal{F} variables (e.g. $m_{ES} > 5.272$ GeV/ c^2 or $\mathcal{F} > -0.1$) to study the stability of the results. The probability density functions (PDFs) introduced to describe the signal, continuum, and K/π misidentification components, along with the K/π misidentification yields, are determined using events from signal and $B^{\mp} \rightarrow D^{(*)}\pi^{\mp}$, $Da_1(1260)^{\mp}$ control samples. The PDFs for $B\bar{B}$ background events are obtained from large Monte Carlo (MC) samples with full detector simulations [9].

The CP fit yields 896 ± 35 (154 ± 14), 255 ± 21 (56 ± 11), 193 ± 19 (30 ± 7), and 163 ± 18 (28 ± 6) signal DK^{\mp} , $D^{*}[D\pi^0]K^{\mp}$, $D^{*}[D\gamma]K^{\mp}$, and $DK^{*\mp}$ events, respectively, for the $K_s^0 \pi^+ \pi^-$ ($K_s^0 K^+ K^-$) final state. The results for the CP -violating parameters $z_{\pm}^{(*)}$ and $z_{s\pm}$ are summarized in Table I. Figure 1 shows the 39.3% and 86.5% 2-dimensional confidence-level (CL) contours in the z_{\mp} , z_{\mp}^* , and $z_{s\mp}$ planes, corresponding to one- and two-standard deviation regions, including statistical errors only. The distance between the z_- and z_+ central values (and similarly for z_{\mp}^* and $z_{s\mp}$) is equal to $2r_{B^{\mp}} |\sin \gamma|$, and the angle defined by the lines connecting the central values with the origin is 2γ , and thus is a measurement of direct CP violation. Fitting separately the data for $K_s^0 \pi^+ \pi^-$ and $K_s^0 K^+ K^-$ final states we find

consistent results for all the CP -violating parameters [11].

TABLE I: CP -violating complex parameters $z_{\mp}^{(*)} = x_{\mp}^{(*)} + iy_{\mp}^{(*)}$ and $z_{s\mp} = x_{s\mp} + iy_{s\mp}$ as obtained from the CP fit. The first error is statistical, the second is the experimental systematic uncertainty and the third is the systematic uncertainty associated with the D^0 decay amplitude models.

| | Real part (%) | Imaginary part (%) |
|----------|---------------------------------|--------------------------------|
| z_- | $6.0 \pm 3.9 \pm 0.7 \pm 0.6$ | $6.2 \pm 4.5 \pm 0.4 \pm 0.6$ |
| z_+ | $-10.3 \pm 3.7 \pm 0.6 \pm 0.7$ | $-2.1 \pm 4.8 \pm 0.4 \pm 0.9$ |
| z_-^* | $-10.4 \pm 5.1 \pm 1.9 \pm 0.2$ | $-5.2 \pm 6.3 \pm 0.9 \pm 0.7$ |
| z_+^* | $14.7 \pm 5.3 \pm 1.7 \pm 0.3$ | $-3.2 \pm 7.7 \pm 0.8 \pm 0.6$ |
| z_{s-} | $7.5 \pm 9.6 \pm 2.9 \pm 0.7$ | $12.7 \pm 9.5 \pm 2.7 \pm 0.6$ |
| z_{s+} | $-15.1 \pm 8.3 \pm 2.9 \pm 0.6$ | $4.5 \pm 10.6 \pm 3.6 \pm 0.8$ |

Experimental systematic errors [9, 11] originate from uncertainties in the description of the efficiency variations across the DP, the modeling of the DP distributions for background events containing misreconstructed D mesons, the fractions of continuum and $B\bar{B}$ background events containing a real D meson with either a negatively- or positively-charged kaon (or K^*), and from residual direct CP violation in the $B^{\mp} \rightarrow D^{(*)}\pi^{\mp}$ and $B\bar{B}$ background components. We also account for statistical and systematic uncertainties in the m_{ES} , ΔE , and \mathcal{F} PDF shapes for signal and background components, and the K/π misidentification yields. These uncertainties account for effects that arise from the dependence of the m_{ES} and \mathcal{F} PDF shapes on the chosen ΔE signal region, the differences in $B\bar{B}$ background for real and misreconstructed D mesons, and our limited knowledge of the m_{ES} endpoint, the peaking contributions to the small $B\bar{B}$ background, and the e^+e^- c.m. frame. Smaller systematic uncertainties originate from the DP resolution, wrongly reconstructed signal events with a real D and a kaon (or K^*) from the other B meson decay, the selection of B candidates sharing tracks with other candidates, and numerical precision in the evaluation of the PDF integrals. We also account for residual cross-feed of $B^{\mp} \rightarrow D^{*}[D\pi^0]K^{\mp}$ events into the $B^{\mp} \rightarrow D^{*}[D\gamma]K^{\mp}$ sample (about 5%), and the estimated uncertainty on the hadronic parameter $\kappa = 0.9 \pm 0.1$ in the $B^{\mp} \rightarrow DK^{*\mp}$ sample [9, 21].

Assumptions in the D^0 decay amplitude models are also a source of systematic uncertainty [9, 11, 12]. We use alternative $\mathcal{A}(s_-, s_+)$ models where the BW parameters are varied according to their uncertainties or within the ranges allowed by measurements from other experiments, the reference K-matrix solution [9] is replaced by other solutions [14], and the standard parameterizations are substituted by other related choices. These include replacing the Gounaris-Sakurai and $K\pi$ S-wave parameterizations by BW lineshapes, removing the mass dependence in the P-vector [22], changes in form factors such as

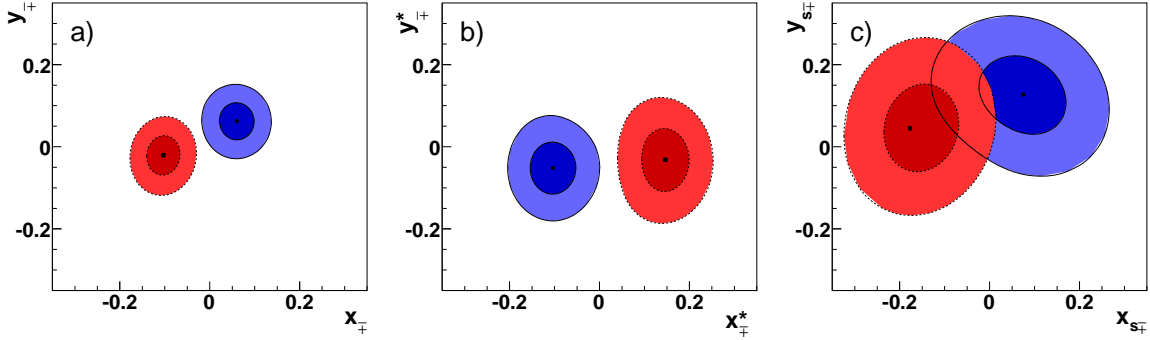


FIG. 1: (color online). Contours at 39.3% (dark) and 86.5% (light) 2-dimensional CL in the (a) z_{\mp} , (b) z_{\mp}^* , and (c) $z_{s\mp}$ planes, corresponding to one- and two-standard deviation regions (statistical only), for B^- (solid lines) and B^+ (dotted lines) decays.

changes in the Blatt-Weisskopf radius, and adopting a helicity formalism [13] to describe the angular dependence. Other models are built by removing or adding resonances with small or negligible fractions. We find that the overall amplitude model uncertainty on the CP parameters are dominated by alternative models built to account for experimental systematic effects in the determination of $\mathcal{A}(s_-, s_+)$ using tagged D mesons [12]. The statistical errors and variations in the $\mathcal{A}(s_-, s_+)$ model parameters with and without D^0 - \bar{D}^0 mixing are also propagated to $z_{\mp}^{(*)}$ and $z_{s\mp}$.

Experimental and amplitude model systematic uncertainties [11] have been reduced with respect to our previous measurement [9] as consequence of the use of larger data and Monte Carlo samples, and the smaller experimental systematic contributions to the model uncertainty resulting from the improvements in the analysis of tagged D mesons [12].

A frequentist construction of 1-dimensional confidence intervals of the physically relevant parameters $\mathbf{p} \equiv (\gamma, r_B, r_B^*, \kappa r_s, \delta_B, \delta_B^*, \delta_s)$ based on the vector of measurements $\mathbf{z} = (z_-, z_+, z_-^*, z_+^*, z_{s-}, z_{s+})$ and their correlations [11] has been adopted [9]. The procedure takes into account unphysical regions which may arise since we allow B^- and B^+ events to have different $r_{B\mp}^{(*)}$, $r_{s\mp}$ in the \mathbf{z} measurements. Figure 2 shows $1 - CL$ as a function of γ for each of the three B decay channels separately and their combination. Similar scans for $r_B^{(*)}$, κr_s , $\delta_B^{(*)}$, and δ_s can be found in [11]. The method has a single ambiguity in the weak and strong phases. The results for all the \mathbf{p} parameters are listed in Table II. The significances of direct CP violation ($\gamma \neq 0$) are $1 - CL = 6.8 \times 10^{-3}$, 5.4×10^{-3} , 6.3×10^{-2} , and 4.6×10^{-4} , which correspond to 2.7, 2.8, 1.9, and 3.5 standard deviations, for $B^\mp \rightarrow DK^\mp$, $B^\mp \rightarrow D^*K^\mp$, $B^\mp \rightarrow DK^{*\mp}$, and their combination, respectively.

We have presented a measurement of the $b \rightarrow u$ to $b \rightarrow c$ complex amplitude ratios in the processes $B^\mp \rightarrow D^{(*)}K^\mp$ and $B^\mp \rightarrow DK^{*\mp}$, using a combined DP

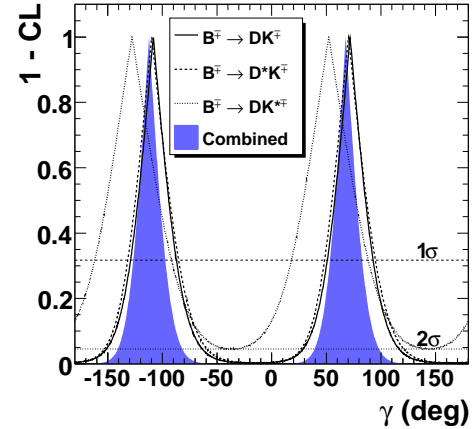


FIG. 2: (color online). $1 - CL$ as a function of γ for $B^\mp \rightarrow DK^\mp$, $B^\mp \rightarrow D^*K^\mp$, and $B^\mp \rightarrow DK^{*\mp}$ decays separately, and their combination, including statistical and systematic uncertainties. The dashed (upper) and dotted (lower) horizontal lines correspond to the one- and two-standard deviation intervals, respectively.

TABLE II: The 68.3% and 95.4% 1-dimensional CL regions, equivalent to one- and two-standard deviation intervals, for γ , $\delta_B^{(*)}$, δ_s , $r_B^{(*)}$, and κr_s , including all sources of uncertainty. The values inside {} brackets indicate the symmetric error contributions to the total error coming from experimental and amplitude model systematic uncertainties.

| Parameter | 68.3% CL | 95.4% CL |
|---------------------------|-----------------------------------|-------------|
| γ ($^\circ$) | $68_{-14}^{+15} \{4, 3\}$ | [39, 98] |
| r_B (%) | $9.6 \pm 2.9 \{0.5, 0.4\}$ | [3.7, 15.5] |
| r_B^* (%) | $13.3_{-3.9}^{+4.2} \{1.3, 0.3\}$ | [4.9, 21.5] |
| κr_s (%) | $14.9_{-6.2}^{+6.6} \{2.6, 0.6\}$ | < 28.0 |
| δ_B ($^\circ$) | $119_{-20}^{+19} \{3, 3\}$ | [75, 157] |
| δ_B^* ($^\circ$) | $-82 \pm 21 \{5, 3\}$ | [-124, -38] |
| δ_s ($^\circ$) | $111 \pm 32 \{11, 3\}$ | [42, 178] |

analysis of $D \rightarrow K_s^0\pi^+\pi^-$ and $D \rightarrow K_s^0K^+K^-$ decays. The results have improved precision and are consistent with our previous measured values [9] and with those reported by the Belle Collaboration with $D \rightarrow K_s^0\pi^+\pi^-$ alone [10], and with determinations based on other D meson final states [21, 23, 24]. From our measurement we determine $\gamma = (68 \pm 14 \pm 4 \pm 3)^\circ$ (modulo 180°), exclude the no direct CP -violation hypothesis (i.e., $\gamma = 0$) with a CL equivalent to 3.5 standard deviations, and derive the most precise single determinations of the magnitude ratios $r_B^{(*)}$ and κr_s .

We are grateful for the excellent luminosity and machine conditions provided by our PEP-II colleagues, and for the substantial dedicated effort from the computing organizations that support *BABAR*. The collaborating institutions wish to thank SLAC for its support and kind hospitality. This work is supported by DOE and NSF (USA), NSERC (Canada), CEA and CNRS-IN2P3 (France), BMBF and DFG (Germany), INFN (Italy), FOM (The Netherlands), NFR (Norway), MES (Russia), MICIIN (Spain), STFC (United Kingdom). Individuals have received support from the Marie Curie EIF (European Union), the A. P. Sloan Foundation (USA) and the Binational Science Foundation (USA-Israel).

(1980); I. I. Bigi and A. I. Sanda, Phys. Lett. B **211**, 213 (1988).

- [4] The symbol D (D^*) indicates either a D^0 (D^{*0}) or a \bar{D}^0 (\bar{D}^{*0}) meson.
- [5] Reference to the charge-conjugate state is implied here and throughout the text unless otherwise specified.
- [6] M. Gronau and D. London, Phys. Lett. B **253**, 483 (1991); M. Gronau and D. Wyler, Phys. Lett. B **265**, 172 (1991); D. Atwood, I. Dunietz and A. Soni, Phys. Rev. Lett. **78**, 3257 (1997); Phys. Rev. D **63**, 036005 (2001); A. Giri, Y. Grossman, A. Soffer and J. Zupan, Phys. Rev. D **68**, 054018 (2003).
- [7] $K^{*\mp}$, $D^{*\mp}$, and D^{*0} refer to $K^*(892)^\mp$, $D^*(2010)^\mp$, and $D^*(2007)^0$ mesons, respectively.
- [8] B. Aubert *et al.* (*BABAR* Collaboration), Nucl. Instrum. Methods Phys. Res., Sect. A **479**, 1 (2002).
- [9] B. Aubert *et al.* (*BABAR* Collaboration), Phys. Rev. D **78**, 034023 (2008); Phys. Rev. Lett. **95**, 121802 (2005).
- [10] A. Poluektov *et al.* (*Belle* Collaboration), Phys. Rev. D **81**, 112002 (2010); Phys. Rev. D **73**, 112009 (2006).
- [11] See supplementary material for additional plots and tables.
- [12] P. del Amo Sanchez *et al.* (*BABAR* Collaboration), Phys. Rev. Lett. **105**, 081803 (2010).
- [13] See review on Dalitz plot Analysis Formalism in C. Amssler *et al.*, Phys. Lett. B **667**, 1 (2008).
- [14] V. V. Anisovich and A. V. Sarantsev, Eur. Phys. Jour. **A16**, 229 (2003).
- [15] D. Aston *et al.* (*LASS* Collaboration), Nucl. Phys. B **296**, 493 (1988); W. Dunwoodie, private communication.
- [16] M. Gronau, Phys. Lett. B **557**, 198 (2003).
- [17] B. Aubert *et al.* (*BABAR* Collaboration), Phys. Rev. D **73**, 111104(R) (2006).
- [18] L. M. Zhang *et al.* (*Belle* Collaboration), Phys. Rev. Lett. **99**, 131803 (2007).
- [19] Y. Grossman, A. Soffer, J. Zupan, Phys. Rev. D **72**, 031501 (2005).
- [20] A. Bondar and T. Gershon, Phys. Rev. D **70**, 091503 (2004).
- [21] B. Aubert *et al.* (*BABAR* Collaboration), Phys. Rev. D **80**, 092001 (2009).
- [22] I. J. R. Aitchison, Nucl. Phys. A **189**, 417 (1972).
- [23] P. del Amo Sanchez (*BABAR* Collaboration), arXiv:1007.0504, to appear in Phys. Rev. D ; arXiv:1006.4241, to appear in Phys. Rev. D ; B. Aubert *et al.* (*BABAR* Collaboration), Phys. Rev. D **78**, 092002 (2008).
- [24] K. Abe *et al.* (*Belle* Collaboration), Phys. Rev. D **73**, 051106(R) (2006); Y. Horii *et al.* (*Belle* Collaboration), Phys. Rev. D **78**, 071901(R) (2008); T. Aaltonen *et al.* (*CDF* Collaboration), Phys. Rev. D **81**, 031105(R) (2010).

* Now at Temple University, Philadelphia, Pennsylvania 19122, USA

† Also with Università di Perugia, Dipartimento di Fisica, Perugia, Italy

‡ Also with Università di Roma La Sapienza, I-00185 Roma, Italy

§ Now at University of South Alabama, Mobile, Alabama 36688, USA

¶ Also with Università di Sassari, Sassari, Italy

** Also with University of Oxford, Theoretical Physics Department, Oxford, OX1 3NP, United Kingdom

[1] N. Cabibbo, Phys. Rev. Lett. **10**, 531 (1963); M. Kobayashi and T. Maskawa, Prog. Theor. Phys. **49**, 652 (1973).

[2] Y. Grossman, M. P. Worah, Phys. Lett. B **395**, 241 (1997); J. Charles *et al.*, Eur. Phys. Jour. C **41**, 1 (2005) and updates at <http://ckmfitter.in2p3.fr/>; F. J. Botella, G. C. Branco, M. Nebot, Nucl. Phys. B **768**, 1 (2007); M. Bona *et al.*, JHEP **803**, 049 (2008) and updates at <http://www.utfit.org/>.

[3] A. B. Carter and A. I. Sanda, Phys. Rev. Lett. **45**, 952

**Evidence for direct CP violation in the measurement of the CKM angle γ with
 $B^\mp \rightarrow D^{(*)} K^{(*)\mp}$ decays**
The BABAR Collaboration

The following includes supplementary material for the Electronic Physics Auxiliary Publication Service.

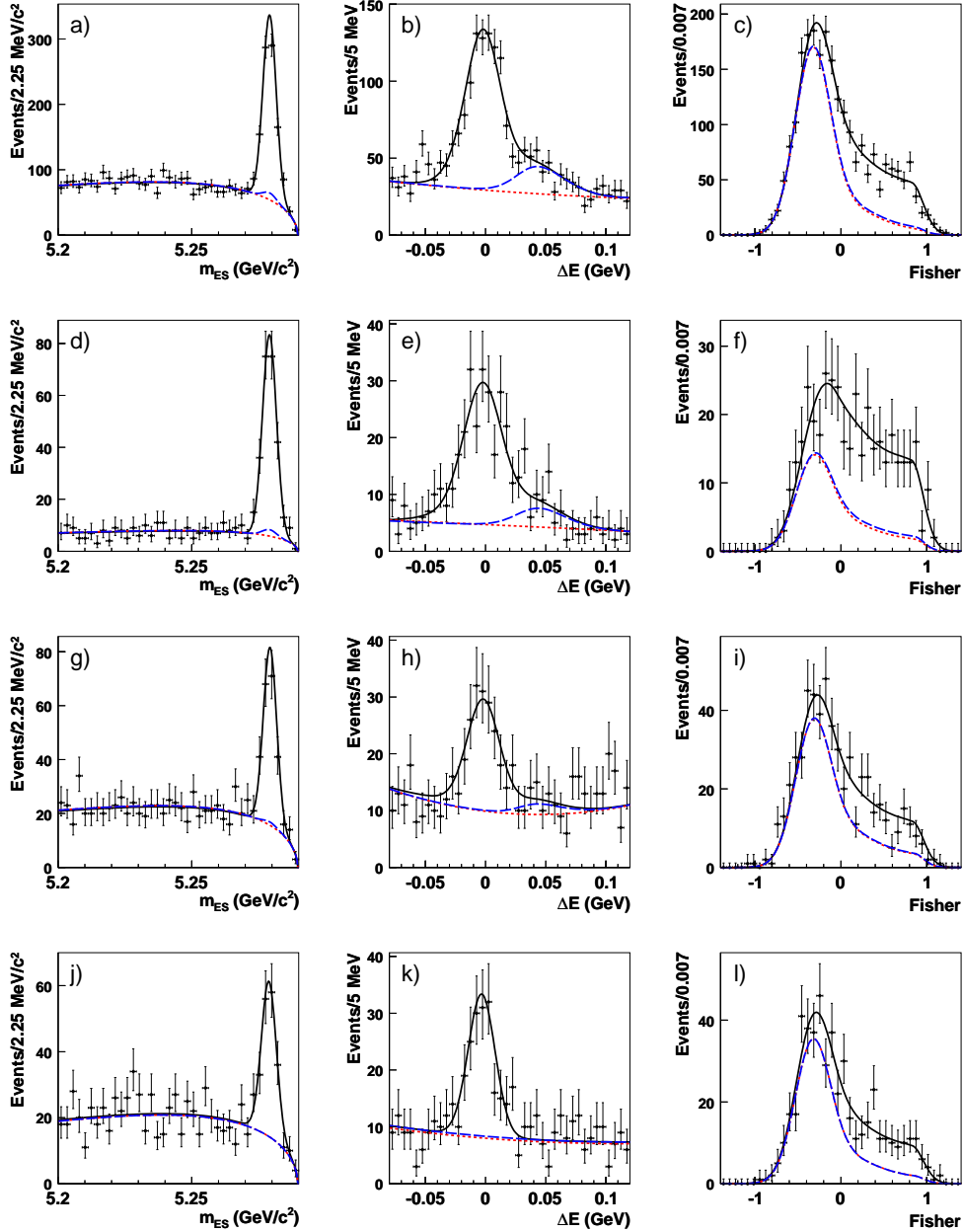


FIG. 1: (color online). The m_{ES} (first column), ΔE (second column), and \mathcal{F} (third column) distributions for (a)-(c) $B^\mp \rightarrow DK^\mp$, (d)-(f) $B^\mp \rightarrow D^*[D\pi^0]K^\mp$, (g)-(i) $B^\mp \rightarrow D^*[D\gamma]K^\mp$, and (j)-(l) $B^\mp \rightarrow DK^{*\mp}$ decays, with $D \rightarrow K_S^0\pi^+\pi^-$. The distributions are for events in the signal region defined through the requirements $m_{ES} > 5.272$ GeV/ c^2 , $|\Delta E| < 30$ MeV, and $\mathcal{F} > -0.1$, except the one on the plotted variable, after all the selection criteria are applied. The curves superimposed represent the projections of the CP fit: signal plus background (solid black lines), the continuum plus $B\bar{B}$ background contributions (dotted red lines), and the sum of the continuum, $B\bar{B}$, and K/π misidentification background components (dashed blue lines). The reconstruction efficiencies (purities) in the signal region, based on simulation studies, are 22% (68%), 10% (81%), 12% (55%), and 12% (58%), respectively.

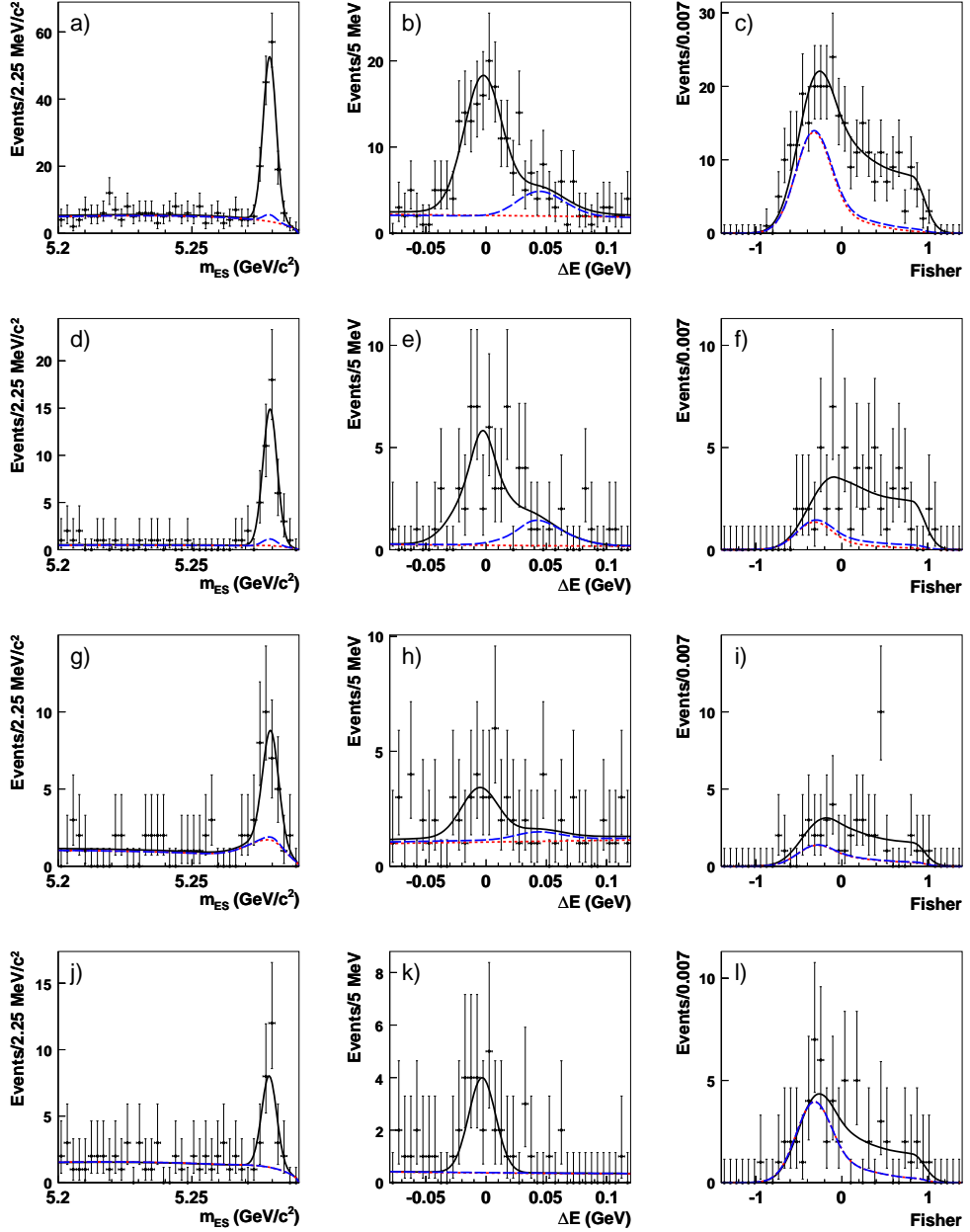


FIG. 2: (color online). Same as in Fig. 1 but for (a)-(c) $B^\mp \rightarrow DK^\mp$, (d)-(f) $B^\mp \rightarrow D^*[D\pi^0]K^\mp$, (g)-(i) $B^\mp \rightarrow D^*[D\gamma]K^\mp$, and (j)-(l) $B^\mp \rightarrow DK^{*\mp}$ decays, with $D \rightarrow K_S^0 K^+ K^-$. The reconstruction efficiencies (purities) in the signal region, based on simulation studies, are in this case 20% (82%), 9% (87%), 12% (78%), and 11% (81%), respectively.

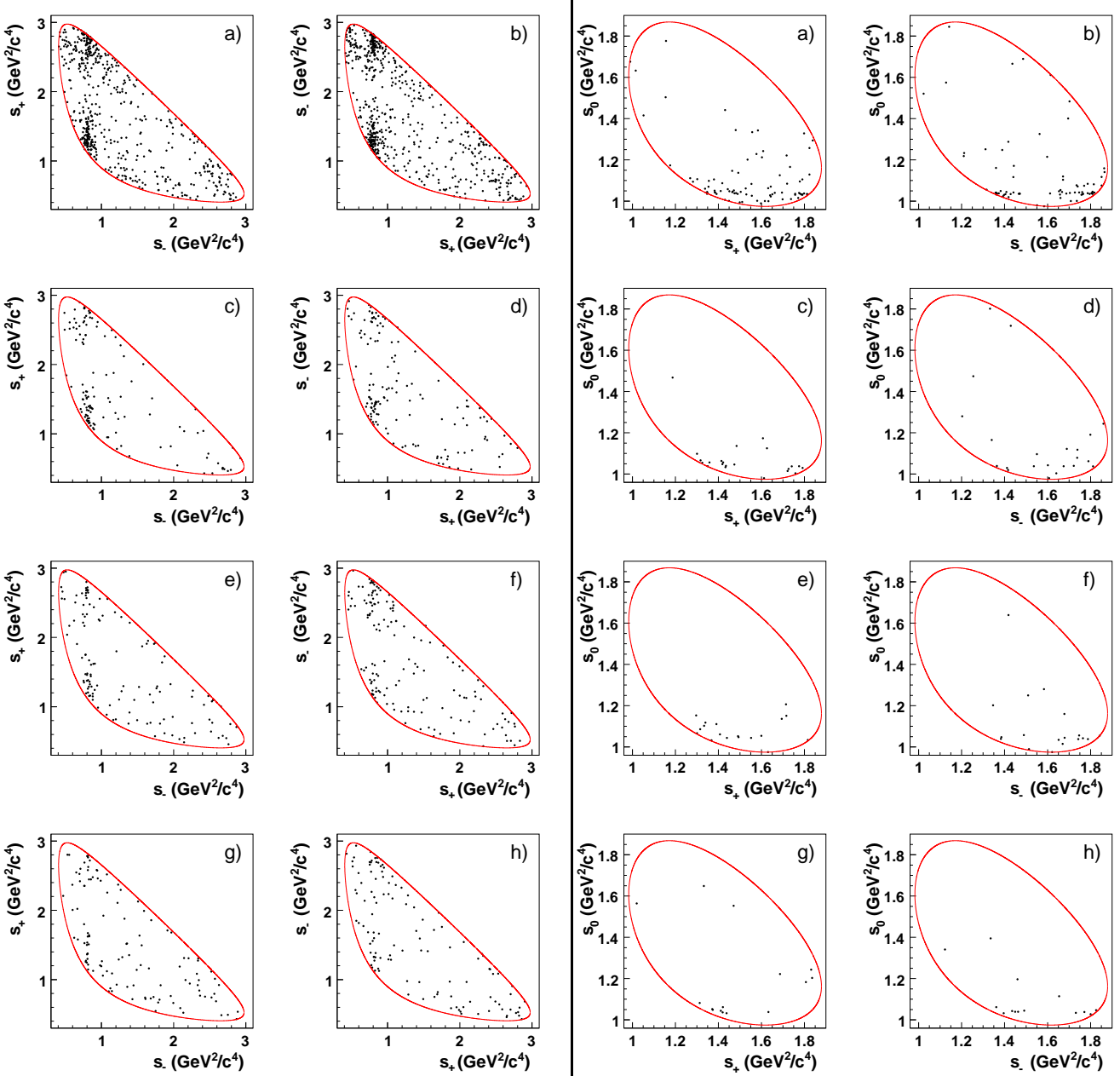


FIG. 3: (color online). The DP distributions for (a)(b) $B^\mp \rightarrow DK^\mp$, (c)(d) $B^\mp \rightarrow D^*[D\pi^0]K^\mp$, (e)(f) $B^\mp \rightarrow D^*[D\gamma]K^\mp$, and (g)(h) $B^\mp \rightarrow DK^{*\mp}$ decays, with $D \rightarrow K_S^0\pi^+\pi^-$ (left panel) and $D \rightarrow K_S^0K^+K^-$ (right panel). The distributions are for events in the signal region defined through the requirements $m_{ES} > 5.272$ GeV/\$c^2\$, $|\Delta E| < 30$ MeV, and $\mathcal{F} > -0.1$, after all the selection criteria are applied, and are shown separately for B^- (first and third columns) and B^+ (second and last column) decays. For B^- and B^+ decays the variables s_- and s_+ are interchanged. The contours (solid red lines) represent the kinematical limits of the D decay.

TABLE I: Summary of the main contributions to the experimental systematic error on the CP parameters. All contributions have been evaluated using the same procedure as in our previous analysis [9]. The statistical contribution to the total error has been decreased, as consequence of the use of larger data and Monte Carlo (with full detector simulation) samples. For example, larger simulated continuum samples help to significantly reduce the uncertainty arising from the modeling of the DP distributions for background events containing misreconstructed D mesons.

| Source | x_- | y_- | x_+ | y_+ | x_-^* | y_-^* | x_+^* | y_+^* | x_{s-} | y_{s-} | x_{s+} | y_{s+} |
|--|-------|-------|-------|-------|---------|---------|---------|---------|----------|----------|----------|----------|
| $m_{ES}, \Delta E, \mathcal{F}$ shapes | 0.001 | 0.001 | 0.001 | 0.001 | 0.004 | 0.006 | 0.008 | 0.004 | 0.006 | 0.003 | 0.004 | 0.002 |
| Real D^0 fractions | 0.002 | 0.001 | 0.001 | 0.001 | 0.003 | 0.003 | 0.002 | 0.002 | 0.004 | 0.001 | 0.001 | 0.001 |
| Charge-flavor correlation | 0.003 | 0.003 | 0.002 | 0.001 | 0.005 | 0.005 | 0.008 | 0.002 | 0.001 | 0.001 | 0.003 | 0.001 |
| Efficiency in the DP | 0.003 | 0.001 | 0.003 | 0.001 | 0.001 | 0.001 | 0.001 | 0.001 | 0.003 | 0.001 | 0.002 | 0.001 |
| Background DP distributions | 0.005 | 0.002 | 0.005 | 0.003 | 0.003 | 0.002 | 0.004 | 0.004 | 0.010 | 0.004 | 0.007 | 0.002 |
| $B^- \rightarrow D^{*0} K^-$ cross-feed | — | — | — | — | 0.002 | 0.003 | 0.009 | 0.002 | — | — | — | — |
| CP violation in $D\pi$ and $B\bar{B}$ | 0.002 | 0.001 | 0.001 | 0.001 | 0.017 | 0.001 | 0.008 | 0.004 | 0.017 | 0.002 | 0.011 | 0.001 |
| Non- K^* $B^- \rightarrow DK_S^0 \pi^-$ decays | — | — | — | — | — | — | — | — | 0.020 | 0.026 | 0.025 | 0.036 |
| Total experimental | 0.007 | 0.004 | 0.006 | 0.004 | 0.019 | 0.009 | 0.017 | 0.008 | 0.029 | 0.027 | 0.029 | 0.036 |

TABLE II: Summary of the main contributions to the D^0 decay amplitude model systematic uncertainty on the CP parameters. We evaluate the different contributions using a similar, but not identical, procedure to that adopted in our previous analysis [9]. The reference D^0 decay amplitude models and parameters are used to generate 10 data-sized signal samples of pseudo-experiments of $D^{*+} \rightarrow D^0 \pi^+$ and $D^{*-} \rightarrow \bar{D}^0 \pi^-$ events, and 10 $B^\mp \rightarrow D^{(*)} K^\mp$ and $B^\mp \rightarrow D K^{*\mp}$ signal samples 100 times larger than each measured signal yield in data, with $D^0 \rightarrow K_S^0 h^+ h^-$. The CP parameters are generated with values in the range found in data. We then compare experiment-by-experiment the values of $z_\mp^{(*)}$ and $z_{s\mp}$ obtained from the CP fits using the reference amplitude models and a set of alternative models obtained by repeating the $D^0 \rightarrow K_S^0 h^+ h^-$ amplitude analyses on the pseudo-experiments with alternative assumptions [12]. This technique, although it requires large computing resources, helps to reduce statistical contributions to the amplitude model uncertainties arising from changes in sensitivity between alternative models (e.g. alternative K-matrix solutions and P-vector mass dependence in the $\pi\pi$ S-wave parameterization). A variety of studies using data have been performed to test the consistency of the results using this procedure with those obtained in our previous analysis, where the alternative models were obtained by repeating the $D^0 \rightarrow K_S^0 h^+ h^-$ amplitude analyses on data. Nevertheless, the largest decrease in the amplitude model uncertainty compared to our previous result is a consequence of the improvements in the experimental analysis of tagged D mesons [12], which is reflected in smaller experimental systematic uncertainties on the D^0 decay amplitudes (variations of the reconstruction efficiency across the DP, modeling of the DP distributions for background events containing misreconstructed D mesons, mistag rates, etc.), and thus smaller amplitude model uncertainties on the CP parameters.

| Source | x_- | y_- | x_+ | y_+ | x_-^* | y_-^* | x_+^* | y_+^* | x_{s-} | y_{s-} | x_{s+} | y_{s+} |
|-----------------------------------|-------|-------|-------|-------|---------|---------|---------|---------|----------|----------|----------|----------|
| Mass and width of Breit-Wigner's | 0.001 | 0.001 | 0.001 | 0.002 | 0.001 | 0.002 | 0.001 | 0.002 | 0.001 | 0.002 | 0.001 | 0.002 |
| $\pi\pi$ S-wave parameterization | 0.001 | 0.001 | 0.001 | 0.001 | 0.001 | 0.001 | 0.001 | 0.002 | 0.001 | 0.001 | 0.001 | 0.002 |
| $K\pi$ S-wave parameterization | 0.001 | 0.004 | 0.003 | 0.008 | 0.001 | 0.006 | 0.002 | 0.004 | 0.003 | 0.002 | 0.003 | 0.007 |
| Angular dependence | 0.001 | 0.001 | 0.002 | 0.001 | 0.001 | 0.001 | 0.001 | 0.002 | 0.002 | 0.001 | 0.002 | 0.001 |
| Blatt-Weisskopf radius | 0.001 | 0.001 | 0.001 | 0.001 | 0.001 | 0.001 | 0.001 | 0.001 | 0.001 | 0.001 | 0.002 | 0.001 |
| Add/remove resonances | 0.001 | 0.001 | 0.001 | 0.001 | 0.001 | 0.002 | 0.001 | 0.001 | 0.001 | 0.001 | 0.001 | 0.002 |
| DP efficiency | 0.003 | 0.002 | 0.003 | 0.001 | 0.001 | 0.001 | 0.001 | 0.001 | 0.004 | 0.002 | 0.003 | 0.001 |
| Background DP shape | 0.001 | 0.001 | 0.001 | 0.001 | 0.001 | 0.001 | 0.001 | 0.001 | 0.001 | 0.001 | 0.001 | 0.001 |
| Mistag rate | 0.003 | 0.003 | 0.002 | 0.001 | 0.001 | 0.001 | 0.001 | 0.001 | 0.003 | 0.003 | 0.001 | 0.001 |
| Effect of mixing | 0.003 | 0.001 | 0.003 | 0.001 | 0.001 | 0.001 | 0.001 | 0.001 | 0.003 | 0.001 | 0.003 | 0.001 |
| DP complex amplitudes | 0.001 | 0.001 | 0.001 | 0.002 | 0.001 | 0.001 | 0.001 | 0.002 | 0.002 | 0.001 | 0.001 | 0.002 |
| Total D^0 decay amplitude model | 0.006 | 0.006 | 0.007 | 0.009 | 0.002 | 0.007 | 0.003 | 0.006 | 0.007 | 0.006 | 0.006 | 0.008 |

TABLE III: CP -violating complex parameters $\mathbf{z}_{\mp}^{(*)} = x_{\mp}^{(*)} + iy_{\mp}^{(*)}$ and $\mathbf{z}_{s\mp} = x_{s\mp} + iy_{s\mp}$ as obtained from the CP fit to $K_S^0\pi^+\pi^-$ and $K_S^0K^+K^-$ final states separately. The first error is statistical, the second is the experimental systematic uncertainty and the third is the systematic uncertainty associated with the D^0 decay amplitude models. These results yield for the weak phase $\gamma = (61^{+19}_{-17})^\circ \{3, 3\}^\circ$ and $\gamma = (87^{+43}_{-37})^\circ \{8, 3\}^\circ$, respectively.

| | $K_S^0\pi^+\pi^-$ | | | | $K_S^0K^+K^-$ | | | |
|----------|---------------------------------|--|---------------------------------|--|----------------------------------|--|-----------------------------------|--|
| | Real part (%) | | Imaginary part (%) | | Real part (%) | | Imaginary part (%) | |
| z_- | $3.6 \pm 4.6 \pm 0.9 \pm 0.6$ | | $6.7 \pm 4.9 \pm 0.4 \pm 0.6$ | | $12.6 \pm 7.6 \pm 1.5 \pm 0.5$ | | $4.4 \pm 11.7 \pm 2.3 \pm 1.2$ | |
| z_+ | $-8.3 \pm 4.1 \pm 0.7 \pm 0.8$ | | $-0.8 \pm 4.9 \pm 0.4 \pm 1.0$ | | $-19.0 \pm 8.7 \pm 2.2 \pm 0.5$ | | $-2.0 \pm 18.8 \pm 6.0 \pm 1.5$ | |
| z^* | $-8.9 \pm 5.8 \pm 1.7 \pm 0.2$ | | $-7.1 \pm 6.8 \pm 0.9 \pm 0.7$ | | $-17.0 \pm 11.0 \pm 2.0 \pm 0.4$ | | $8.8 \pm 17.1 \pm 3.6 \pm 1.2$ | |
| z_+^* | $15.4 \pm 5.9 \pm 1.4 \pm 0.4$ | | $-3.6 \pm 8.7 \pm 0.9 \pm 0.7$ | | $11.7 \pm 11.7 \pm 4.2 \pm 0.4$ | | $-2.5 \pm 16.4 \pm 1.9 \pm 0.5$ | |
| z_{s-} | $12.8 \pm 10.5 \pm 3.4 \pm 0.8$ | | $12.0 \pm 10.5 \pm 2.5 \pm 0.6$ | | $-11.7 \pm 20.8 \pm 8.2 \pm 0.8$ | | $14.3 \pm 22.4 \pm 9.5 \pm 1.4$ | |
| z_{s+} | $-9.6 \pm 9.2 \pm 3.2 \pm 0.8$ | | $3.8 \pm 10.9 \pm 3.7 \pm 0.9$ | | $-36.6 \pm 20.1 \pm 5.8 \pm 0.6$ | | $-17.1 \pm 39.9 \pm 13.5 \pm 1.7$ | |

TABLE IV: Statistical correlation coefficients for the vector \mathbf{z} of measurements, (in order) x_- , y_- , x_+ , y_+ , x_-^* , y_-^* , x_+^* , y_+^* , x_{s-} , y_{s-} , x_{s+} , y_{s+} , as obtained from the CP fit to $K_S^0\pi^+\pi^-$ and $K_S^0K^+K^-$ final states (upper panel), and to $K_S^0\pi^+\pi^-$ (bottom left panel) and $K_S^0K^+K^-$ (bottom right panel) separately. Only lower off-diagonal terms are written, in %.

$$\begin{array}{c} \left(\begin{array}{cccccccccc} 100 & & & & & & & & & \\ -2 & 100 & & & & & & & & \\ 0 & 0 & 100 & & & & & & & \\ 0 & 0 & 6 & 100 & & & & & & \\ 0 & 0 & 0 & 0 & 100 & & & & & \\ 0 & 0 & 0 & 0 & -1 & 100 & & & & \\ 0 & 0 & 0 & 0 & 0 & 0 & 100 & & & \\ 0 & 0 & 0 & 0 & 0 & 0 & -3 & 100 & & \\ 0 & 0 & 0 & 0 & 0 & 0 & 0 & 0 & 100 & \\ 0 & 0 & 0 & 0 & 0 & 0 & 0 & 0 & -20 & 100 \\ 0 & 0 & 0 & 0 & 0 & 0 & 0 & 0 & 0 & 100 \\ 0 & 0 & 0 & 0 & 0 & 0 & 0 & 0 & 0 & 10 \\ \end{array} \right) \\ \left(\begin{array}{cccccccccc} 100 & & & & & & & & & \\ -4 & 100 & & & & & & & & \\ 0 & 0 & 100 & & & & & & & \\ 0 & 0 & 4 & 100 & & & & & & \\ 0 & 0 & 0 & 0 & 100 & & & & & \\ 0 & 0 & 0 & 0 & 4 & 100 & & & & \\ 0 & 0 & 0 & 0 & 0 & 0 & 100 & & & \\ 0 & 0 & 0 & 0 & 0 & 0 & -7 & 100 & & \\ 0 & 0 & 0 & 0 & 0 & 0 & 0 & 0 & 100 & \\ 0 & 0 & 0 & 0 & 0 & 0 & 0 & 0 & -18 & 100 \\ 0 & 0 & 0 & 0 & 0 & 0 & 0 & 0 & 0 & 100 \\ 0 & 0 & 0 & 0 & 0 & 0 & 0 & 0 & 0 & 0 \\ 0 & 0 & 0 & 0 & 0 & 0 & 0 & 0 & 0 & 0 \\ \end{array} \right) \left(\begin{array}{cccccccccc} 100 & & & & & & & & & \\ 5 & 100 & & & & & & & & \\ 0 & 0 & 100 & & & & & & & \\ 0 & 0 & 13 & 100 & & & & & & \\ 0 & 0 & 0 & 0 & 100 & & & & & \\ 0 & 0 & 0 & 0 & -10 & 100 & & & & \\ 0 & 0 & 0 & 0 & 2 & 0 & 100 & & & \\ 0 & 0 & 0 & 0 & 0 & 0 & 15 & 100 & & \\ 0 & 0 & 0 & 0 & 0 & 0 & 0 & 0 & 100 & \\ 0 & 0 & 0 & 0 & 0 & 0 & 0 & 0 & -19 & 100 \\ 0 & 0 & 0 & 0 & 0 & 0 & 0 & 0 & 0 & 100 \\ 0 & 0 & 0 & 0 & 0 & 0 & 0 & 0 & 0 & -7 & 100 \\ \end{array} \right) \end{array}$$

TABLE V: Experimental systematic correlation coefficients for the vector \mathbf{z} of measurements, (in order) $x_-, y_-, x_+, y_+, x_-^*, y_-^*, x_+^*, y_+^*, x_{s-}, y_{s-}, x_{s+}, y_{s+}$, defined as $\rho_{ij} = \mathcal{C}_{ij}/\sqrt{\mathcal{C}_{ii}\mathcal{C}_{jj}}$, where $\mathcal{C}_{ij} = \overline{(\mathbf{z} - \mathbf{z}_{\text{best}})_i(\mathbf{z} - \mathbf{z}_{\text{best}})_j}$, with \mathbf{z}_{best} the vector of best measurements, for $K_S^0\pi^+\pi^-$ and $K_S^0K^+K^-$ final states (upper panel), and $K_S^0\pi^+\pi^-$ (bottom left panel) and $K_S^0K^+K^-$ (bottom right panel) separately. Only lower off-diagonal terms are written, in %.

$$\begin{pmatrix} 100 \\ -23 & 100 \\ -2 & 18 & 100 \\ -5 & -5 & 0 & 100 \\ -32 & -10 & -13 & 5 & 100 \\ -15 & 13 & -2 & -5 & -2 & 100 \\ -12 & -9 & -9 & 5 & 44 & -60 & 100 \\ 12 & 17 & 16 & -9 & -50 & 19 & -44 & 100 \\ -19 & -8 & -15 & -7 & 49 & 0 & 25 & -25 & 100 \\ 3 & -6 & -3 & -3 & -8 & -5 & -2 & 5 & 63 & 100 \\ -20 & 0 & -7 & 0 & 33 & 0 & 16 & -14 & 73 & 65 & 100 \\ -1 & -6 & -3 & 0 & -3 & -4 & -3 & 2 & 66 & 97 & 74 & 100 \end{pmatrix} \quad \begin{pmatrix} 100 \\ -72 & 100 \\ -78 & 59 & 100 \\ -91 & 78 & 88 & 100 \\ -41 & 30 & 17 & 34 & 100 \\ 10 & -11 & -12 & -5 & -52 & 100 \\ -2 & -11 & -7 & -1 & 60 & -52 & 100 \\ -20 & 47 & 1 & 19 & 44 & -42 & 46 & 100 \\ -13 & 5 & -8 & 3 & -1 & -2 & 3 & 9 & 100 \\ 12 & -6 & 6 & -4 & 7 & 2 & 0 & -6 & -98 & 100 \\ -25 & 32 & 40 & 36 & 7 & 15 & -12 & 3 & -80 & 81 & 100 \\ 16 & -21 & -31 & -26 & -16 & 0 & 2 & -5 & 85 & -85 & -95 & 100 \end{pmatrix}$$

TABLE VI: Amplitude model systematic correlation coefficients for the vector \mathbf{z} of measurements, (in order) $x_-, y_-, x_+, y_+, x_-^*, y_-^*, x_+^*, y_+^*, x_{s-}, y_{s-}, x_{s+}, y_{s+}$, defined as previously, for $K_S^0\pi^+\pi^-$ and $K_S^0K^+K^-$ final states (upper panel), and $K_S^0\pi^+\pi^-$ (bottom left panel) and $K_S^0K^+K^-$ (bottom right panel) separately. Only lower off-diagonal terms are written, in %.

$$\begin{pmatrix} 100 \\ 9 & 100 \\ 83 & -31 & 100 \\ 25 & -56 & 57 & 100 \\ 28 & -64 & 71 & 61 & 100 \\ 6 & -74 & 44 & 93 & 64 & 100 \\ 24 & 80 & -15 & -74 & -50 & -86 & 100 \\ 0 & 51 & -15 & -74 & -16 & -76 & 74 & 100 \\ 86 & -23 & 91 & 54 & 52 & 39 & -12 & -22 & 100 \\ 11 & 85 & -20 & -18 & -54 & -41 & 52 & 16 & -11 & 100 \\ 77 & -38 & 96 & 61 & 73 & 50 & -23 & -18 & 91 & -26 & 100 \\ 30 & -51 & 56 & 95 & 56 & 89 & -70 & -77 & 53 & -14 & 58 & 100 \end{pmatrix} \quad \begin{pmatrix} 100 \\ 48 & 100 \\ 22 & -36 & 100 \\ -33 & -48 & 23 & 100 \\ -36 & -82 & 53 & 56 & 100 \\ -52 & -84 & 38 & 57 & 88 & 100 \\ 43 & 40 & -5 & -31 & -41 & -47 & 100 \\ 29 & 36 & -16 & -31 & -42 & -45 & 30 & 100 \\ 59 & 49 & 6 & -33 & -42 & -53 & 37 & 26 & 100 \\ 42 & 86 & -35 & -43 & -77 & -80 & 33 & 29 & 46 & 100 \\ 75 & 66 & 4 & -44 & -57 & -70 & 49 & 39 & 62 & 59 & 100 \\ -49 & -69 & 33 & 56 & 81 & 83 & -48 & -49 & -48 & -60 & -66 & 100 \end{pmatrix}$$

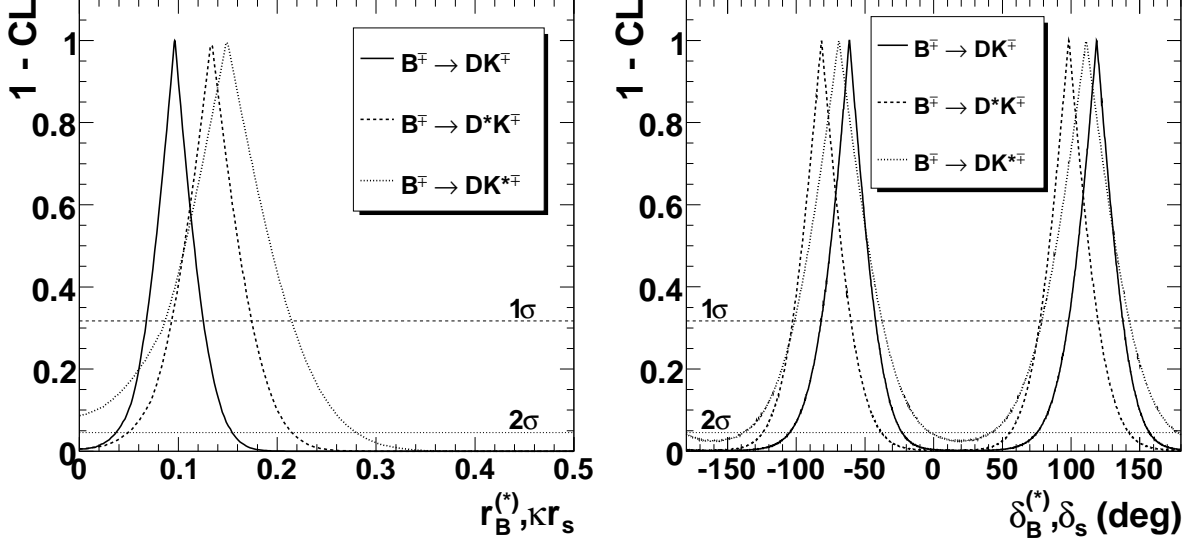


FIG. 4: $1 - \text{CL}$ as a function of (left panel) r_B , r_B^* , and κr_s , and (right panel) δ_B , δ_B^* , and δ_s , for $B^\mp \rightarrow DK^\mp$, $B^\mp \rightarrow D^*K^\mp$, and $B^\mp \rightarrow DK^{*\mp}$ decays, including statistical and systematic uncertainties. The dashed (upper) and dotted (lower) horizontal lines correspond to the one- and two-standard deviation intervals, respectively.

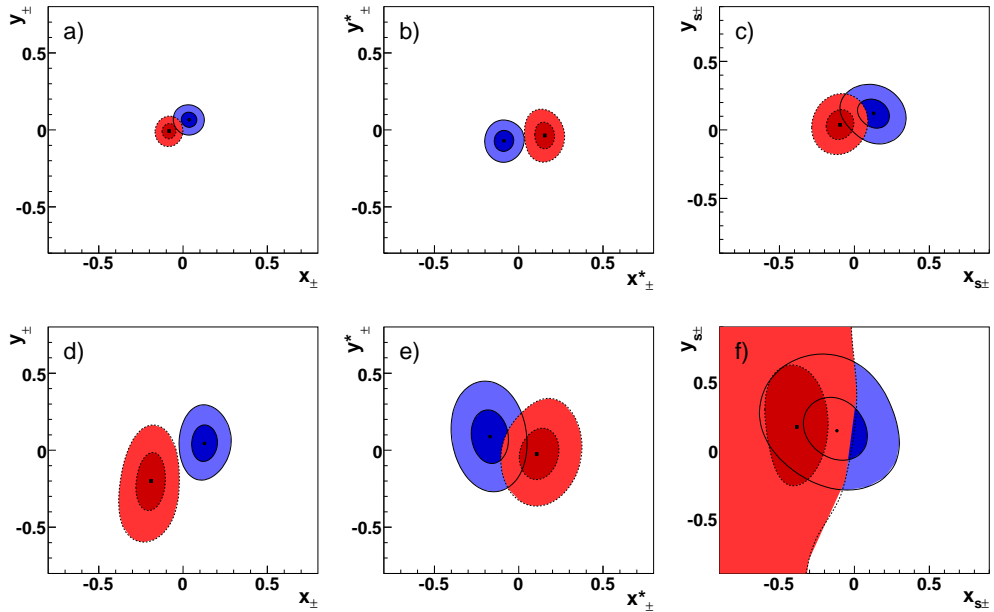


FIG. 5: (color online). Contours at 39.3% (dark) and 86.5% (light) 2-dimensional CL in the (a)(d) z_\pm , (b)(e) z_\pm^* , and (c)(f) $z_{s\pm}$ planes, corresponding to one- and two-standard deviation regions (statistical only), for B^- (solid lines) and B^+ (dotted lines) decays, from the CP fit to the signal samples performed separately for (a)-(c) $D \rightarrow K_S^0 \pi^+ \pi^-$ and (d)-(f) $D \rightarrow K_S^0 K^+ K^-$ decays. The results from the two subsets are statistically consistent.

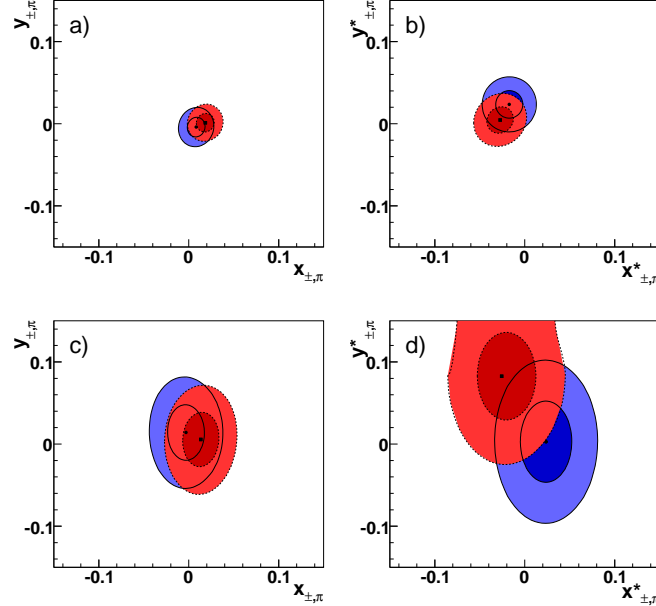


FIG. 6: (color online). Contours at 39.3% (dark) and 86.5% (light) 2-dimensional CL in the (a)(c) $z_{\mp,\pi}$ and (b)(d) $z_{\mp,\pi}^*$ planes, corresponding to one- and two-standard deviation regions (statistical only), for B^- (solid lines) and B^+ (dotted lines) decays, from the CP fit to the $B^\mp \rightarrow D^{(*)}\pi^\mp$ control samples performed separately for (a)(b) $D \rightarrow K_S^0\pi^+\pi^-$ and (c)(d) $D \rightarrow K_S^0K^+K^-$ decays. In this case we expect the $z_{\mp,\pi}$ and $z_{\mp,\pi}^*$ contours close to the origin up to ~ 0.01 , since $r_{B,\pi}^{(*)} \approx 0.01$ and the experimental resolutions are of the same order. Deviations from this pattern could be an indication that the DP distributions are not well described by the amplitude models [9]. The results from all the subsets are consistent with the expectations. Note the differences in scale when comparing to Fig. 5.